

Nongray Particulate Radiation in an Isothermal Cylindrical Medium

J. D. Felske
Assistant Professor.

K. M. Lee¹
Student.

Department of Mechanical Engineering,
State University of New York at Buffalo,
Amherst, NY 14260

The radial radiative heat flux and its divergence are determined both exactly and approximately for homogeneous suspensions of small particles. Scattering is assumed to be small compared to absorption and the absorption coefficient is taken to be inversely proportional to wavelength. The exact solution is reduced to an infinite series of single integrals. The optically thin and the next higher order behavior appear in closed form as the first two terms in the series. Two approximate solutions are also developed. One is in good agreement with the exact solution while the other is not. Finally, a closed form approximate relation is derived for the dimensionless heat flux at the surface. This expression, which also gives the emissivity or absorptivity of the medium, is in excellent agreement with the exact result.

Introduction

The equations describing the radiative heat transfer in an infinitely long cylindrical medium are well known [1, 2]. Using the radial radiative flux formulation of [2], several investigators have studied radiative transfer in nongray gaseous media having discrete absorption bands [3-10]. In [3-5] radiation was taken to be the only mode of energy transfer while in [6-10] combined modes were considered. Nongray continuum radiation due to particulates is also an important contributor to the total radiative transfer in combustion systems [11]. Depending upon the fuel and how it is burned, the importance of this particulate radiation will range from insignificant to dominant. Under all conditions, however, the radiation from the combined gas/particulate mixture may be analyzed in a way such that one term in the solution represents particulate radiation in the absence of any gaseous participation [12]. Hence, the nongray problem concerning a purely particulate medium is of fundamental importance to combined gas/particulate analyses. In [13] the problem of particulate radiation in a parallel plate geometry was considered. Approximate closed form solutions for nonhomogeneous media were developed there. The purpose of the present work is to develop exact and approximate results for isothermal particle suspensions in the more common combustion geometry—cylindrical.

Exact Solution

The particles produced in the combustion of hydrocarbon fuels are often small enough such that the radiative interchange may be predicted using the small particle limit of Mie's equations. In this limit and for these absorbing particles, scattering is negligible and the spectral absorption coefficient is reasonably approximated by [13].

$$k = C/\lambda \quad (1)$$

where $C = c_0 f_v$, in which f_v is the local volume fraction of particles and c_0 is a constant whose value lies between 3 and 7. In the following analysis, the particle concentration will be assumed spatially uniform and hence C will be constant.

The spectral, radial radiative heat flux is given in [2] for the general case wherein the temperature and absorption coefficient are allowed to vary with radius across the cylindrical medium. Using this spectral result, the total radial flux for a homogeneous nongray particulate medium having an absorption coefficient given by equation (1) may be written as

$$q''(r) = 4 \int_0^\infty I_{b\lambda}(T_w) \int_0^{\pi/2} \cos \gamma D_3(x_1) d\gamma d\lambda \\ - 4 \int_0^\infty I_{b\lambda}(T_w) \int_0^{\pi/2} \cos \gamma D_3(x_2) d\gamma d\lambda$$

¹ Presently, graduate student at M.I.T.

Contributed by the Heat Transfer Division for publication in the JOURNAL OF HEAT TRANSFER. Manuscript received by the Heat Transfer Division February 29, 1980.

$$+ 4C \int_0^\infty \lambda^{-1} I_{b\lambda}(T_g) \int_0^{\pi/2} \cos \gamma \int_r^{r_0} D_2(x_3) \\ \times \frac{dr'}{\cos \gamma'} d\gamma d\lambda \quad (2)$$

$$+ 4C \int_0^\infty \lambda^{-1} I_{b\lambda}(T_g) \int_0^{\pi/2} \cos \gamma \int_r^r D_2(x_4) \frac{dr'}{\cos \gamma'} d\gamma d\lambda \\ - 4C \int_0^\infty \lambda^{-1} I_{b\lambda}(T_g) \int_0^{\pi/2} \cos \gamma \int_r^{r_0} D_2(x_5) \frac{dr'}{\cos \gamma'} d\gamma d\lambda$$

where $I_{b\lambda}(T)$ is Planck's blackbody intensity function and

$$x_1 = Cr_0 \lambda^{-1} \{ [1 - (r/r_0)^2 \sin^2 \gamma]^{1/2} + (r/r_0) \cos \gamma \} \\ x_2 = Cr_0 \lambda^{-1} \{ [1 - (r/r_0)^2 \sin^2 \gamma]^{1/2} - (r/r_0) \cos \gamma \} \\ x_3 = Cr' \lambda^{-1} \{ [1 - (r/r')^2 \sin^2 \gamma]^{1/2} + (r/r') \cos \gamma \} \\ x_4 = Cr' \lambda^{-1} \{ [1 - (r/r')^2 \sin^2 \gamma]^{1/2} - (r/r') \cos \gamma \} \\ x_5 = -x_4 \quad (3)$$

and

$$D_n(x) = \int_0^1 \mu^{n-1} (1 - \mu^2)^{-1/2} \exp(-x/\mu) d\mu \quad (4)$$

The terms in equation (2) represent the following heat flows. The first term is the contribution to the radially outward flux at point P (see Fig. 1) from wall emission at points like B . The exponential quantity in this term (which appears through D_3) is the transmittance for the line of sight from B to P . Wall emission from points like A which gets transmitted to point P is accounted for in the second term. Since this flow is radially inward, the term is negative. The third and fourth terms are contributions to the radially outward flux resulting from local particulate emission which is transmitted to point P . The third

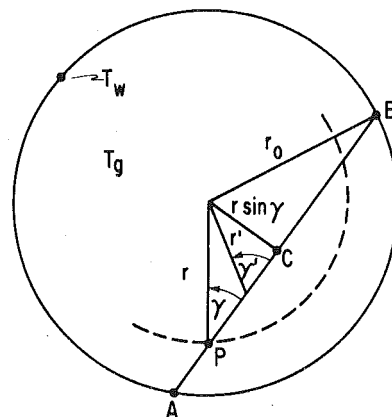


Fig. 1 Fundamental pathlengths for the cylindrical geometry

term accounts for such emission along the path from B to C while the fourth term accounts for the section from C to P . The last term in the equation is the local particulate emission along the line of sight AP which is transmitted to point P . It is radially inward and hence it is negative.

The complexity of the integrals does not allow an exact closed form solution to be obtained. Nevertheless, several of the integrals may be performed analytically. This greatly reduces the numerical computation burden and, in addition, allows the optically thin and the next higher order behavior to be achieved in closed form—appearing as the first two terms in the infinite series solution. The transformations leading to the closed form integrations are presented in detail in [14]; a brief outline is given below.

Initially, either the r' or the λ integration may be performed. It was found, however, that performing the λ integration first allows the problem to be pursued further on an analytical basis. (The direction into which the solution proceeds when the r' integration is completed first can be seen from the modified gray result given in the next section.) Letting $x \equiv 1/\lambda$, the spectral integrals in equation (2) may be cast into the form of Riemann's zeta function $\zeta(\nu, \mu/\beta)$. The key in being able to go beyond this first integration and achieve further analytical reduction lies in then expressing the zeta function as an infinite series [15].

$$\begin{aligned} \zeta(\nu, \mu/\beta) &= \frac{\beta^\nu}{\Gamma(\nu)} \int_0^\infty \frac{x^{\nu-1} e^{-\mu x}}{1-e^{-\beta x}} dx \\ &= \sum_{n=0}^{\infty} (\mu/\beta + n)^{-\nu} \end{aligned} \quad (5)$$

Using this series representation and defining

$$\begin{aligned} k &= \frac{r}{r_0}; \quad p = \frac{Cr_0 T_w}{C_2}; \quad q = \frac{Cr_0 T_g}{C_2} \\ \beta_{1r} &= \frac{(1+n)/\tau}{k \cos \gamma + \sqrt{1-k^2 \sin^2 \gamma}}; \\ \beta_{2r} &= \frac{(1+n)/\tau}{-k \cos \gamma + \sqrt{1-k^2 \sin^2 \gamma}}; \\ \beta_3 &= \frac{(1+n)/q}{k \cos \gamma + \sqrt{(r'/r_0)^2 - k^2 \sin^2 \gamma}}; \\ \beta_4 &= \frac{(1+n)/q}{k \cos \gamma - \sqrt{(r'/r_0)^2 - k^2 \sin^2 \gamma}} = -\beta_5 \end{aligned} \quad (7)$$

in which τ will be either p or q , the expression for the radial heat flux may be written as

$$\begin{aligned} q''(r) &= 48C_1 C_2^{-4} T_w^4 \sum_{n=0}^{\infty} \int_0^{\pi/2} \cos \gamma \\ &\quad \left\{ \int_0^1 [f_4(\beta_{1p}) - f_4(\beta_{2p})] d\mu \right\} d\gamma \\ &+ 192CC_1 C_2^{-5} T_g^5 \sum_{n=0}^{\infty} \int_0^{\pi/2} \cos \gamma \int_0^1 \left\{ \int_{r \sin \gamma}^{r_0} f_5(\beta_3) dr'/\cos \gamma' \right. \\ &\quad \left. + \int_{r \sin \gamma}^r f_5(\beta_4) dr'/\cos \gamma' - \int_r^{r_0} f_5(\beta_5) dr'/\cos \gamma' \right\} d\mu d\gamma \end{aligned} \quad (8)$$

where

$$f_m(\beta) = \frac{\mu^6}{(1-\mu^2)^{1/2}} \left[\frac{\beta}{(1+n)(1+\beta\mu)} \right]^m \quad m = 4, 5 \quad (9)$$

In the second term in the above equation the three integrations with respect to r' are the same. Each may be completed in closed form by first expressing $dr'/\cos \gamma'$ in terms of the β_j ($j = 3, 4, 5$). (It should be noted from Fig. 1 that $r \sin \gamma = r' \sin \gamma'$ and hence $\cos \gamma' = [1 - (r/r')^2 \sin^2 \gamma]^{1/2}$.) Then the integrations with respect to μ may be completed in closed form by first using trigonometric substitutions followed by partial fraction expansions. The $G_m(\beta)$ functions which appear in the final result below are generated at this point.

The remaining integrations with respect to γ may be completed analytically only when the integrands do not contain the $G_m(\beta)$ functions. Those integrations which can be completed are then able to be summed exactly through the definition of the Riemann zeta function, equation (5). The resulting expression for the radial radiative heat flux then becomes

$$q''(k) = F(q, k) \sigma T_g^4 - F(p, k) \sigma T_w^4 \quad (10)$$

where

$$F(\tau, k) = c_1 k \tau - c_2 k f_1(k^2) \tau^2 + R(\tau, k) \quad (11)$$

in which

$$\begin{aligned} R(\tau, k) &= \frac{3 \cdot 5^1}{\pi^5} \sum_{n=0}^{\infty} \frac{1}{(1+n)^4} \int_{\gamma=0}^{\pi/2} \sum_{m=1}^4 (-1)^{m+1} (4 \frac{6}{m}) \\ &\quad \times \left\{ \frac{G_m(\beta_{1r})}{\beta_{1r}^2} - \frac{G_m(\beta_{2r})}{\beta_{2r}^2} \right\} \cos \gamma d\gamma \end{aligned} \quad (12)$$

and

$$f_1(k^2) = \frac{4}{\pi} \int_{\gamma=0}^{\pi/2} \cos^2 \gamma (1 - k^2 \sin^2 \gamma)^{1/2} d\gamma \quad (13)$$

Closed form expressions for the $G_m(\beta)$ functions are given in the Appendix. The function $f_1(k^2)$ may be identified as the hypergeometric function ${}_2F_1(-1/2, 1/2; 2; k^2)$. It decreases monotonically from $f_1(0) = 1.00$ to $f_1(1) = 0.85$ and has very little curvature. The constants c_1 and c_2 have the values $c_1 = 6! \zeta(5)/\pi^4 = 7.664$ and $c_2 = 15 \cdot 5! \zeta(6)/\pi^3 = 59.06$.

The solution is therefore seen to be governed by the single function $F(\tau, k)$. That this should be the case is certainly not obvious upon inspection of equation (8). It is, however, clear on physical grounds since for an isothermal medium the radial flux must vanish at all radii when the wall and medium temperatures are equal. The fact that $F \neq F(p, q, k)$ is a consequence of the spectral absorption coefficient being independent of temperature (see equation (1)). As a result, the mean absorption coefficient of the medium for wall emission is independent of the temperature of the medium. Hence the second term in equation (10), which is the part of the emitted wall energy which is absorbed by the medium in the region $0 \leq r' \leq r$, is a function of the wall temperature but not the medium temperature. Similarly, the radially outward emission of energy by the medium (the first term in equation (10)) is independent of the wall temperature. The fact that $p \propto T_w$ and $q \propto T_g$ results from the mean absorption and emission coefficients being linearly dependent upon the temperature of the sources of radiation [13]. This linearity in temperature stems solely

Nomenclature

a_n, b_n = coefficients in $D_n(x)$ approximation

C = particle concentration parameter

C_1, C_2 = first and second radiation constants

$D_n(x) = \int_0^1 \mu^{n-1} (1-\mu^2)^{-1/2} \exp(-x/\mu) d\mu$

F, F_g, F_d = fundamental functions for the exact, gray, and approximate $D_n(x)$ results, respectively

${}_2F_1$ = Gauss' hypergeometric function

$f_1(k^2) = {}_2F_1(-1/2, 1/2; 2; k^2)$

$f_2(k^2) = {}_2F_1(1/2, 3/2; 3; k^2)$

$I_{b\lambda w}$ = Wien's distribution

k = dimensionless radius

k_m = mean absorption or emission coefficient

k_λ = spectral absorption coefficient

p, q = optical depths for wall and medium emission

q'', q_g'', q_d'' = exact, gray and approximate

$D_n(x)$ heat fluxes, respectively

Q = remainder function in div F

R = remainder function in F

r, r_0 local radius and tube radius

T, T_g, T_w = general, medium and wall temperatures, respectively

ζ = Riemann's zeta function

λ = wavelength

σ = Stefan-Boltzmann constant

τ = optical depth

from the λ^{-1} variation of the spectral absorption coefficient since the radiative properties of the particles themselves are assumed independent of temperature.

The Function $F(\tau, k)$. The first two terms in equation (11) appear to be the beginning of a series expansion for $F(\tau, k)$ in terms of the optical depth τ . This observation may be verified by determining the optically thin behavior of the function $R(\tau, k)$. Substituting equations (36) and (39) of the Appendix into equation (12) and taking the limit as $\tau \rightarrow 0$, it can be shown that

$$R(\tau, k) = g_1(k)\tau^3 \ln(1/\tau) - g_2(k)\tau^3 \quad \tau \ll 1 \quad (14)$$

where the functions $g_1(k)$ and $g_2(k)$ are of the order of magnitude 10. Hence for $\tau \ll 1$ it is seen that $R(\tau, k)$ is negligible compared to the first two terms in $F(\tau, k)$, thereby demonstrating that these terms are a valid expansion for $F(\tau, k)$ in the optically thin region. From numerical computations it was found that $F(\tau, k)$ may be determined to within one percent by using simply the first term in equation (11) when $\tau \lesssim 10^{-3}$ and by using only the first two terms when $\tau \lesssim 10^{-2}$. The third term, $R(\tau, k)$, initially achieves importance at small τ as a result of the first two becoming of the same magnitude but of opposite sign. At large τ the first term is much smaller than either of the last two. However, all three terms are important since the second and third terms are of equal magnitude but opposite sign. Therefore, when $\tau \gtrsim 10^{-2}$ all terms must be retained in the computation.

Figure 2 presents the function $F(\tau, k)$. A simple physical interpretation of its behavior is obtained by noting that when $T_w = 0$ K the radial flux is only a consequence of medium emission: $q''(k) = F(q, k)\sigma T_g^4$. Under optically thin conditions, energy emitted within the cylinder $0 \leq r' \leq r$ escapes from it without being absorbed. Similarly, energy emitted within the surrounding annulus $r \leq r' \leq r_0$ passes through the cylinder region without being absorbed. The net radially outward flux at r is then simply equal to the total energy emitted within the cylindrical region (proportional to its volume) divided by the surface area of the region: $q''(r) = 4(V/A)k_p\sigma T_g^4$, in which k_p is the Planck mean emission coefficient. For media composed of small particles whose spectral absorption characteristics are given by equation (1), it was shown in [13] that $k_p = 3.83 CT_g/C_2$. Hence in the optically thin limit, $F(\tau, k) = 7.67k$. This result is also predicted by equation (11). The linear proportionality with respect to both τ and k in this limit may be seen in Fig. 2.

Deviation from linearity occurs for $\tau > 10^{-3}$. This is a result of two physical effects. First, of the energy emitted within the cylinder region some is absorbed internally and therefore not all escapes. Hence, the radial flux due to this emission increases at a slower rate with optical

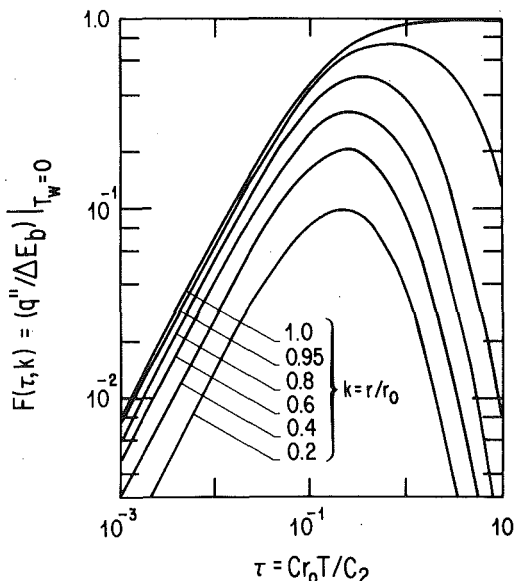


Fig. 2 The single function which determines the radial flux. Also the dimensionless flux when $T_w = 0$

depth than in the optically thin region. Secondly, radiation from the surrounding annular region no longer passes completely through the cylinder region but experiences progressively greater absorption in it as the optical depth increases. This, then, contributes an inward radial flux—directly reducing the net outward flux. At the surface of the medium ($r = r_0$) where there is no inward flux for $T_w = 0$, the net flux simply increases with optical depth (at an ever diminishing rate of increase) until blackbody emission is asymptotically achieved. However, at points internal to the medium ($r < r_0$), the ever increasing inward flux (due to increasing absorption in the cylinder region of the increasing emission from the annular region) counterbalances the outward emitted flux. The tradeoff causes a maximum in net radial flux to be achieved. As the optical depth is increased, the annular emission approaches blackbody radiation at temperature T_g and all of it is absorbed within the cylinder region. The energy emitted within the cylinder region also becomes blackbody at T_g and it is absorbed within the annulus. As a result, the net flux, and hence $F(\tau, k)$, go to zero.

The Function $\text{div } F(\tau, k)$. When determining the temperature and concentration distributions in combustion systems, a first law analysis requires a specification of the divergence of the radiative heat flux. Although the present analysis applies strictly to homogeneous systems (where specification of the flux divergence is clearly unnecessary) the results can nevertheless serve as a first approximation to the radiative transfer in nonhomogeneous systems. Such an approximation is particularly useful when the radiative transfer represents only one part of a complex combustion analysis.

The divergence of the radial heat flux is defined by the single function $\text{div } F(\tau, k)$. This function may be determined by differentiating equation (11) and using the relationship given in equation (40) of the Appendix. The result is

$$r_0 \text{div } F = 2c_1\tau - c_2[2f_1(k^2) - (k^2/4)f_2(k^2)]\tau^2 + Q(\tau, k) \quad (15)$$

where

$$Q(\tau, k) = \frac{3.5!}{\pi^5} \sum_{n=0}^{\infty} \frac{1}{(1+n)^4} \int_{\gamma=0}^{\pi/2} \sum_{m=1}^4 (-1)^{m+1} \times (4 \frac{6}{m}) \left\{ \frac{G_m(\beta_{1\tau})}{\beta_{1\tau}^2} - \frac{G_m(\beta_{2\tau})}{\beta_{2\tau}^2} \right\} + \frac{\tau^2}{(1+n)^2} \nu(1/\rho) [mG_{m+1}(\beta_{1\tau}) - (m+2)G_m(\beta_{1\tau})] - \frac{\tau^2}{(1+n)^2} \nu(\rho) [mG_{m+1}(\beta_{2\tau}) - (m+2)G_m(\beta_{2\tau})] \cos \gamma \, d\gamma \quad (16)$$

in which

$$\nu(x) = 2x[(1+x)^{-1} - (1-k^2)/2] \quad (17)$$

$$\rho = \beta_{1\tau}/\beta_{2\tau} \quad (18)$$

The function $f_2(k^2)$ is the hypergeometric function ${}_2F_1(1/2, 3/2; 3; k^2)$. It increases monotonically from $f_2(0) = 1.00$ to $f_2(1) = 1.70$ and has significant upward curvature.

In the optically thin limit the function $Q(\tau, k)$ has the same form as $R(\tau, k)$, with the corresponding $g_i(k)$ functions being of order 100. In this limit, $Q(\tau, k)$ is therefore negligible compared to the first two terms in equation (15). From numerical computation it was found that $r_0 \text{div } F$ may be determined to within one percent by using only the first term in equation (15) when $\tau \lesssim 10^{-3}$ and by using only the first two terms when $\tau \lesssim 10^{-2}$. This behavior is similar to that of the function $F(\tau, k)$ itself.

Figure 3 presents the function $r_0 \text{div } F(\tau, k)$. As with $F(\tau, k)$ a physical interpretation is facilitated by noting that the function is exactly the flux divergence resulting from medium emission only, i.e., $T_w = 0$ K. In the optically thin limit, there is no self-absorption and all of the energy emitted by a dr element must escape radially. Hence, this emission per unit area (which is directly proportional to optical depth) exactly defines the $\text{div } q''$. Although the energy emitted by each dr element is not the same, the emission per unit area is identical. Hence, in the optically thin limit $r_0 \text{div } F$ must be independent of

radius and directly proportional to optical depth. These trends are seen in Fig. 3 and are predicted by the first term in equation (15). As the optical depth increases, the photon mean free path decreases, and the center of the cylinder becomes the first region unable to see the 0 K environment surrounding the medium. It is therefore the first region which sees an essentially isothermal environment at the temperature T_g . Under these circumstances both q'' and $\text{div } q''$ will decrease in the central region of the cylinder as the optical depth increases. The central region itself will expand with increasing optical depth. Hence, with the surface flux increasing monotonically with optical depth while the flux within the medium is approaching zero at ever larger radii, the $\text{div } q''$ will become larger within an ever narrowing annular region. As the optical depth approaches infinity the central region expands to the surface and the $\text{div } q''$ approaches zero everywhere internal to the cylinder. At the surface, however, the $\text{div } q''$ approaches infinity as a result of the step change in flux across the interface.

$q''(r)$: Exact and Approximate Solutions

The Exact Solution. When either the wall or the medium is cold, equation (11) and Fig. 2 give the dimensionless flux exactly. That is, for $T_w = 0$ or $T_g = 0$, $F(\tau, k) = q''(k)/(\sigma T_g^4 - \sigma T_w^4)$. However, when the wall and medium emissions are both important, equation (10) must be used and the optical depths for both emission and absorption by the medium (q and p respectively) enter the solution. Equivalently, since $p/q = T_w/T_g$ one may consider the parameters q and T_w/T_g as defining the solution at a given radius. It should also be noted that if p and q are interchanged (equivalent to interchanging T_w and T_g) the same value is obtained for the dimensionless flux. Expressions for the heat flux in the optically thin limit may be written by appropriately using the one and two term expressions for $F(\tau, k)$ discussed in the previous section. For example, when both p and q are less than 10^{-3} (equivalently $q \lesssim 10^{-3}$ and $T_w/T_g \lesssim 1.0$) the dimensionless flux is accurately given by

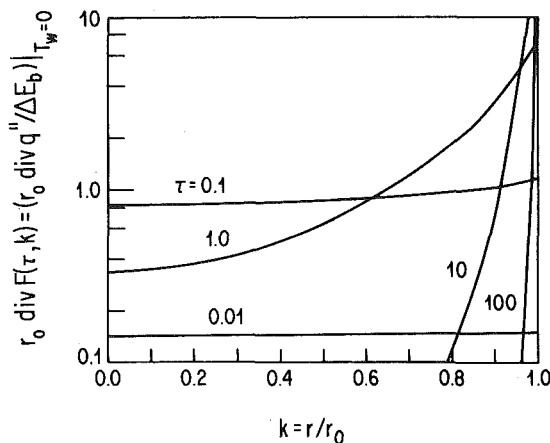


Fig. 3 The single function which determines the flux divergence. Also the dimensionless flux divergence when $T_w = 0$

Table 1 The dimensionless heat flux $q''/\sigma(T_g^4 - T_w^4)$ as computed exactly and by two approximate methods

k	$q = 0.1$			$q = 1.0$			$q = 10.0$		
	$T_w/T_g = 0.0$	1.0 ⁴	10.0	0.0	1.0	10.0	0.0	1.0	10.0
0.2	0.0824 ¹	0.0918	0.0388	0.0357	2.30E-2	1.79E-4	1.83E-4	5.55E-5	1.85E-7
	0.0915 ²	0.1028	0.0180	0.0144	4.37E-3	-1.80E-6	3.27E-15	-7.65E-14	-3.27E-9
	0.0852 ³	0.0954	0.0320	0.0320	1.88E-2	4.74E-5	5.06E-5	5.39E-6	2.40E-9
0.6	0.258	0.290	0.174	0.166	0.121	1.61E-3	1.63E-3	5.45E-4	1.96E-6
	0.284	0.322	0.123	0.111	0.066	-1.22E-5	2.24E-8	-9.62E-8	-2.24E-12
	0.265	0.300	0.157	0.158	0.109	6.24E-4	6.40E-4	4.97E-4	5.82E-8
1.0	0.474	0.548	0.961	0.963	0.980	1.000	1.000	1.000	1.000
	0.514	0.596	0.989	0.992	0.996	1.000	1.000	1.000	1.000
	0.481	0.558	0.972	0.972	0.985	1.000	1.000	1.000	1.000

¹ Exact solution

² Modified gray solution

³ Solution using $D_n(x) = a_n e^{-bnx}$ and Wien's distribution (corrected)

⁴ Values obtained by interpolation between 0.9 and 1.1 results

$$\frac{q''(r)}{\sigma T_g^4 - \sigma T_w^4} = c_1 \left[\frac{1 - (T_w/T_g)^6}{1 - (T_w/T_g)^4} \right] kq \quad (19)$$

The function of the temperature ratio in brackets above increases monotonically with T_w/T_g . It has the values of 1.0 and 1.25 for $(T_w/T_g) = 0, 1.0$ respectively; and it approximately equals (T_w/T_g) for large arguments.

The dimensionless heat flux has been computed exactly from equation (10) in the following parameter ranges: $10^{-5} \leq q \leq 10^3$ and $0.0 \leq (T_w/T_g) \leq 10.0$. When plotted, the results for a fixed temperature ratio always appear similar to Fig. 2 (the dimensionless flux for $T_w/T_g = 0$). The essential difference is that the curve for a given radius shifts toward smaller values of q as T_w/T_g is increased. Plots of the dimensionless flux at various temperature ratios will not be presented. Rather, the results for $q = 0.1, 1.0, 10.0$ are presented in Table 1. The peaks of the curves lie in or near this range of q when $(T_w/T_g) < 10$.

The Gray Approximation. By performing the geometric integrations in equation (2) first, a spectral or gray solution results. The r' integrations may be completed for a medium in which the absorption coefficient is spatially uniform by using the substitution $y = [(r'/r)^2 - \sin^2 \gamma]^{1/2}$ along with its implication $dr'/\cos \gamma' = r dy$. Finally, letting $x = \sin \gamma$ and combining the wall emission terms into a single term and the medium emission terms into a single term, the radial heat flux becomes

$$q_\lambda''(k) = F_g(\tau_\lambda, k) E_{b\lambda}(T_g) - F_g(\tau_\lambda, k) E_{b\lambda}(T_w) \quad (20)$$

where

$$F_g(\tau_\lambda, k) = \frac{4}{\pi} \int_{x=0}^1 \int_{\mu=0}^1 \frac{\mu^2}{(1 - \mu^2)^{1/2}} \left\{ \exp \left[-\frac{\tau_\lambda}{\mu} (\sqrt{1 - k^2 x^2} - k\sqrt{1 - x^2}) \right] - \exp \left[-\frac{\tau_\lambda}{\mu} (\sqrt{1 - k^2 x^2} + k\sqrt{1 - x^2}) \right] \right\} d\mu dx \quad (21)$$

and $\tau_\lambda = k_\lambda r_0$. The above spectral result will also be the solution for the total radiative interchange if the medium is gray and if an appropriate mean absorption coefficient can be defined.

As shown in [13] the Planck and Rosseland mean coefficients corresponding to $k_\lambda = C/\lambda$ have the same form:

$$k_m = BCT/C_2 \quad (22)$$

where B equals 3.83 for the Planck coefficient and 4.00 for the Rosseland. (The value of 3.60 given in [13] for the Rosseland coefficient is in error.) For use over the full range of optical depths it is reasonable to assume a mean value of 3.91. Also, it is noted that since the coefficient k_m is linearly proportional to temperature, the mean emission coefficient (characterized by T_g) will be different from the mean absorption coefficient (characterized by T_w). If this difference is not accounted for, the gray solution will be independent of T_w/T_g . Since this contradicts the nature of the exact solution, the gray result should be modified as follows

$$q_g''(r) = F_g(\tau_g, k) \sigma T_g^4 - F_g(\tau_w, k) \sigma T_w^4 \quad (23)$$

where

$$\tau_g = BCr_0 T_g / C_2 = 3.91 q \quad (24)$$

$$\tau_w = BCr_0 T_w / C_2 = 3.91 p \quad (25)$$

In Table 1, values of the heat flux predicted by the above approximate expression are compared with those computed from the exact solution. The modified gray result predicts the general trend with T_w/T_g but it is somewhat inaccurate. It was found to be in good agreement (≤ 5 percent error) only when $q \leq 0.01$ and $(T_w/T_g) \leq 10$. Additionally, it predicts negative results (which violate the second law) at large optical depths when $T_w/T_g > 0$. (After careful study of such results we are convinced that the negative values stem from the modified gray approximation and not from computational inaccuracies.) A better approximation is clearly desirable.

Approximate Geometric Integration. The second approximate solution investigated here accounts exactly for the nongray properties of the particles and instead performs the geometric integrations in an approximate way. The functions $D_n(x)$ appearing in equation (2) are approximated as $D_n(x) \approx a_n e^{-b_n x}$ after the manner of [3, 4]. In addition, Wien's distribution, $I_{b\lambda w} = 2C_1 \lambda^{-5} \exp(-C_2/\lambda T)$, is used to approximate the Planck function. Introducing these approximations, the spectral integrals acquire the same form as they had in [13]. This, however, is to be expected since the geometric functions of the cylindrical geometry, $D_n(x)$, are being approximated here in the same way as the geometric functions of the planar geometry, $E_n(x)$, were approximated in [13]. Performing these spectral integrations followed by the r' integrations, the following approximate result is obtained for the radial heat flux

$$q_d''(k) = \frac{8C_1 a_2 3!}{b_2 C_2^4} [F_d(\tau_{gd}, k) T_g^4 - (a_3 b_2 / a_2) F_d(\tau_{wd}, k) T_w^4] \quad (26)$$

where

$$F_d(\tau, k) = \int_{\gamma=0}^{\pi/2} \{ [1 + \tau(\sqrt{1 - k^2 \sin^2 \gamma} - k \cos \gamma)]^{-4} - [1 + \tau(\sqrt{1 - k^2 \sin^2 \gamma} + k \cos \gamma)]^{-4} \} \cos \gamma d\gamma \quad (27)$$

and

$$\tau_{gd} = b_2 C r_0 T_g / C_2 = b_2 q \quad (28)$$

$$\tau_{wd} = b_3 C r_0 T_w / C_2 = b_3 p \quad (29)$$

The coefficients in the $D_n(x)$ approximation are taken to be [4]:

$$\begin{aligned} a_2 &= 3\pi^2/32 & a_3 &= \pi/4 \\ b_2 &= 3\pi/8 & b_3 &= 3\pi/8 \end{aligned} \quad (30)$$

As a consequence, $(a_3 b_2 / a_2) = 1.0$, $(8C_1 a_2 3! / b_2 C_2^4) = 0.924 \sigma$. Then, normalizing equation (26) by dividing it by the difference between the hemispherical emissive powers computed from Wien's distribution ($E_{bw} = 0.924 \sigma T^4$), it is seen that the 0.924 coefficient cancels. This automatically corrects for the inherent underprediction of flux embodied in the use of Wien's function. The result is

$$\frac{q''(k)}{\sigma T_g^4 - \sigma T_w^4} \approx \frac{q_d''(k)}{0.924(\sigma T_g^4 - \sigma T_w^4)} = \frac{F_d(\tau_{gd}, k) T_g^4 - F_d(\tau_{wd}, k) T_w^4}{T_g^4 - T_w^4} \quad (31)$$

At the surface of the medium ($k = 1$) the dimensionless flux may be determined in closed form. It is straightforward to show using a table of integrals [15] that

$$F_d(\tau, 1) = 1 + \frac{3 + 20\tau^2 - 8\tau^4}{6(1 - 4\tau^2)^3} \pm \frac{4(\tau^3 \pm \tau)}{(1 - 4\tau^2)^3} G_1(2\tau) \quad (32)$$

where the upper signs are to be used for $2\tau > 1$ and the lower signs for $2\tau < 1$. When $2\tau = 1$, $F_d(0.5, 1) = 0.124$. The function $G_1(\beta)$ is given by equation (36) in the Appendix. It should be noted that the emissivity and absorptivity of the nongray cylindrical medium are given, respectively, by

$$\epsilon = F_d(\tau_{gd}, 1) \quad (33)$$

and

$$\alpha = F_d(\tau_{wd}, 1) \quad (34)$$

The numerical computations in Table 1 show that this approximate solution is quite accurate. The largest errors occur when q or p is large (i.e., when q or (T_w/T_g) is large). This, however, is to be expected since the coefficients in the approximations to the $D_n(x)$ were obtained by requiring accurate representations at short pathlengths [4]. The error introduced by using Wien's distribution is nearly the same for all pathlengths and is much less than the error introduced by the $D_n(x)$ approximation at large pathlengths. The simple closed form solution for the heat flux at the surface given by equation (32) is remarkably accurate over the full range of optical depths.

Conclusions

Exact and approximate solutions have been developed for the radial radiative heat flux in a nongray cylindrical medium. In the exact solution, several of the integrals which originally appear in the formulation have been completed in closed form. The final result appears as an infinite series of integrals in which the first two terms (the optically thin and the next higher order term) are known in closed form. Upper limits on the optical depth have been established below which either the first term or the first two terms in the series will accurately represent the radial heat flux. Similar considerations were also given to the determination of the flux divergence.

In addition, two different approximate solutions have been derived. The first approximates the spectral integrations by assuming that the absorption coefficient is independent of wavelength, i.e., that the medium is gray. The gray result is then modified to allow the mean absorption coefficient to be different from the mean emission coefficient. Nevertheless, good agreement with the exact result is only achieved at small optical depths.

The second approximate solution performs the geometric integration in an approximate way and uses Wien's distribution instead of Planck's in the spectral integrations. The values of the radial heat flux predicted by this result are in good agreement with the exact solution over a much wider range than those of the modified gray result. In addition, a simple closed form expression for the heat flux at the surface is obtained. This expression, which is also the emissivity or absorptivity of the medium, accurately predicts the exact result over the full range of optical pathlengths.

Acknowledgments

This work was supported by grants from the SUNY Research Foundation (Faculty Research Fellowship) and the National Science Foundation (ENG-7825053).

References

- 1 Kuznetsov, Ye. S., "Temperature Distribution in an Infinite Cylinder and in a Sphere in a State of Non-Monochromatic Radiation Equilibrium," English translation in *USSR Computational Mathematics and Mathematical Physics*, Vol. 2, 1963, pp. 230-254.
- 2 Kesten, A. S., "Radiant Heat Flux Distribution in a Cylindrically Symmetric Nonisothermal Gas With Temperature-Dependent Absorption Coefficient," *Journal of Quantitative Spectroscopy and Radiative Transfer*, Vol. 8, 1968, pp. 419-434.
- 3 Habib, I. S., and Greif, R., "Nongray Radiative Transport in a Cylindrical Medium," *ASME JOURNAL OF HEAT TRANSFER*, Vol. 92, 1970, pp. 28-32.
- 4 Wassel, A. T., and Edwards, D. K., "Molecular Gas Band Radiation in Cylinders," *ASME JOURNAL OF HEAT TRANSFER*, 1974, pp. 21-26.
- 5 Nelson, D. A., "Band Radiation within Diffuse-Walled Enclosures; Part I: Exact Solutions for Simple Enclosures," *ASME JOURNAL OF HEAT TRANSFER*, Vol. 101, 1979, pp. 81-84.
- 6 Habib, I. S., and Greif, R., "Heat Transfer to a Flowing Nongray Radiating Gas: an Experimental and Theoretical Study," *International Journal of Heat and Mass Transfer*, Vol. 13, 1970, pp. 1571-1582.
- 7 Tiwari, S. N., and Cess, R. D., "Heat Transfer to Laminar Flow of Nongray Gases Through a Circular Tube," *Applied Scientific Research*, Vol. 25, 1971, pp. 155-170.
- 8 Wassel, A. T., Edwards, D. K., and Catton, I., "Molecular Gas Radiation and Laminar or Turbulent Heat Diffusion in a Cylinder with Internal Heat Generation," *International Journal of Heat and Mass Transfer*, Vol. 18, 1975, pp. 1267-1276.
- 9 Wassel, A. T., and Edwards, D. K., "Molecular Gas Radiation in a

Laminar or Turbulent Pipe Flow," ASME JOURNAL OF HEAT TRANSFER, 1976, pp. 101-107.

10 Greif, R., "Laminar Convection with Radiation: Experimental and Theoretical Results," *International Journal of Heat and Mass Transfer*, Vol. 21, 1978, pp. 477-480.

11 Hottel, H. C., and Sarofim, A. F., *Radiative Transfer*, McGraw-Hill, New York, 1967.

12 Felske, J. D., and Tien, C. L., "Calculation of the Emissivity of Luminous Flames," *Combustion Science and Technology*, Vol. 7, 1973, pp. 25-31.

13 Felske, J. D., and Tien, C. L., "The Use of the Milne-Eddington Absorption Coefficient for Radiative Heat Transfer in Combustion Systems," ASME JOURNAL OF HEAT TRANSFER, Vol. 99, 1977, pp. 458-465.

14 Felske, J. D., and Lee, K. M., "Nongray Particulate Radiation in an Isothermal Cylindrical Medium," Fluid and Thermal Sciences Laboratory, Tech. Rept., TR 80-1, SUNY/Buffalo, Feb 1980.

15 Gradshteyn, I. S., and Ryzhik, I. M., *Table of Integrals, Series and Products*, Academic Press, New York, 1965.

APPENDIX

The $G_m(\beta)$ functions are defined by:

$$G_m(\beta) = \int_{\alpha=0}^{\pi/2} (1 + \beta \cos \alpha)^{-m} d\alpha \quad (35)$$

It is clear from the above equation that $G_0(\beta) = \pi/2$. Using a table of integrals [15] it can be shown that

$$G_1(\beta) = \begin{cases} \frac{2}{(1 - \beta^2)^{1/2}} \tan^{-1} [(1 - \beta^2)^{1/2}/(1 + \beta)], & \beta^2 < 1 \\ (\beta^2 - 1)^{-1/2} \ln \left[\frac{1 + \beta + (\beta^2 - 1)^{1/2}}{1 + \beta - (\beta^2 - 1)^{1/2}} \right], & \beta^2 > 1 \end{cases} \quad (36)$$

with $G_1(1) = 1$. For $m > 1$, the $G_m(\beta)$ functions may be expressed in terms of $G_1(\beta)$ through the recurrence relation derived below. From

[15] it is seen that the integral defining $G_m(\beta)$ may be written as

$$\begin{aligned} & \int_0^{\pi/2} (1 + \beta \cos \alpha)^{-m} d\alpha \\ &= -\frac{1}{(m-1)(1-\beta^2)} \left\{ \beta - (m-1) \int_0^{\pi/2} (1 + \beta \cos \alpha)^{-(m-1)} d\alpha \right. \\ & \quad \left. + (m-2)\beta \int_0^{\pi/2} (1 + \beta \cos \alpha)^{-(m-1)} \cos \alpha d\alpha \right\} \quad (37) \end{aligned}$$

The last term in this equation may be written in terms of $G_m(\beta)$ functions by noting that

$$(1 + \beta \cos \alpha)^{-1} \cos \alpha = [1 - (1 + \beta \cos \alpha)^{-1}]/\beta \quad (38)$$

Substituting the above into equation (37), combining terms and using equation (35), the following relationship is obtained

$$\begin{aligned} G_m(\beta) = & -\frac{1}{(m-1)(1-\beta^2)} [\beta + (m-2)G_{m-2}(\beta) \\ & - (2m-3)G_{m-1}(\beta)] \quad m \geq 2 \quad (39) \end{aligned}$$

For $m > 0$, the $G_m(\beta)$ functions decrease monotonically to zero as β increases. When $\beta = 0$, $G_m(0) = \pi/2$ for all m ; and when $m < n$, $G_m(\beta) > G_n(\beta)$.

In developing the result for $\text{div } F(\tau, k)$, derivatives of the $G_m(\beta)$ functions are required. These derivatives may be expressed in terms of the functions themselves. By taking the derivative of equation (35) and then introducing equation (38), it follows that

$$dG_m(\beta)/d\beta = [G_{m+1}(\beta) - G_m(\beta)]m/\beta \quad (40)$$

Hence the appearance of $G_{m+1}(\beta)$ in equation (16).